CMS Physics Analysis Summary

Contact: cms-pog-conveners-jetmet@cern.ch 2010/11/19

Determination of the Jet Energy Scale in CMS with pp Collisions at $\sqrt{s} = 7$ TeV

The CMS Collaboration

Abstract

The determination of the jet energy calibration in CMS is presented. In-situ measurements are performed using $3\,\mathrm{pb}^{-1}$ of proton-proton collisions at 7 TeV center of mass energy. The transverse momentum balancing in dijet and photon+jet events is used to measure the relative and absolute jet energy response in the CMS detector. Observations in data are compared to Monte Carlo expectations and the systematic uncertainties related to the calibration scheme are discussed. The results are presented for three different approaches to reconstruct jets in the CMS detector: calorimeter-based jet reconstruction; the "Jet-Plus-Track" algorithm, which improves the measurement of calorimeter jets by exploiting the associated tracks; the "Particle Flow" method, which attempts to reconstruct individually each particle in the event, prior to the jet clustering, based on information from all relevant sub-detectors.

1 Introduction

Jets are experimental signatures of quarks and gluons produced in high energy processes such as hard scattering of partons in pp collisions. The detailed understanding of the jet energy calibration is of crucial importance and a leading source of systematic uncertainty for many physics analyses at LHC. This paper presents studies for the determination of the energy scale of jets produced in CMS with pp collisions at $\sqrt{s} = 7\,\text{TeV}$, using $L_{int} \simeq 3\,\text{pb}^{-1}$ of integrated luminosity.

A jet that is reconstructed and measured from the detector inputs (referred to as *detector jet*) has energy that is typically different than that of the corresponding particle jet (also referred to as *generator jet*). The latter is obtained in the simulation by clustering, with the same jet algorithm, the stable particles produced during the hadronization process that follows the hard interaction. The main cause for this energy mismatch is the non-uniform and non-linear response of the CMS calorimeters. Furthermore, electronics noise and additional pp interactions in the same bunch crossing (event pile-up) can lead to extra unwanted energy. The purpose of the jet energy calibration is to relate, on average, the energy measured in the detector jet to the energy of the corresponding particle jet. The correction is applied as a multiplicative factor $C(p_{\text{T}}^{raw}, \eta)$ on each component of the raw jet momentum four-vector P_{μ}^{raw} (components indexed by μ in the following):

$$P_{\mu}^{corrected} = C(p_{\text{T}}^{raw}, \eta) \cdot P_{\mu}^{raw} \tag{1}$$

The success of the CMS simulation in describing jet properties [1] allows its effective use in the jet calibration scheme. The reconstructed jets are first calibrated with a Monte Carlo truth correction and subsequently small residual corrections are applied, based on the in-situ measurements of the relative (vs η) and the absolute (vs p_{T}) jet energy scale.

Results for the jet energy calibration are presented for three different approaches to reconstruct jets in the CMS detector: calorimeter-based jet reconstruction [1] (CALO jets); the "Jet-Plus-Track" algorithm [2], which improves the measurement of calorimeter jets by exploiting the associated tracks (JPT jets); and the "Particle Flow" method [3, 4], which attempts to reconstruct each individual particle in the event, prior to the jet clustering, based on information from all relevant sub-detectors (PF jets). In all three cases jets are clustered using the Anti-k_{T} [5] algorithm. The results presented here correspond mainly to the cone parameter $R = 0.5$ while some measurements, sensitive to the jet size, are also performed for the cone parameter $R = 0.7$.

This paper is organized as follows: Section 2 refers briefly to the Monte Carlo truth calibration, Section 3 describes the determination of the relative jet energy scale vs η and the associated systematic uncertainties. The measurement of the absolute jet energy scale vs p_{T} and its uncertainties are discussed in Section 4. The combined uncertainties from the relative and absolute energy scale are presented in Section 5. Section 6 summarizes the results.

2 Monte Carlo Truth Calibration

The Monte Carlo truth jet energy corrections are derived using QCD simulated events from proton-proton collisions at $\sqrt{s} = 7\,\text{TeV}$. The events are generated with PYTHIA [6] and are further processed through the full GEANT 4 [7] based simulation of the CMS detector. In these events, CALO, JPT, and PF jets are reconstructed, as well as particle jets (generator jets). The generated jets are spatially matched to the reconstructed jets (RecoJets) in the $\eta - \phi$ space by

requiring $\Delta R = \sqrt{(\Delta\eta)^2 + (\Delta\phi)^2} < 0.25$. For the matched jets, the quantity $p_{\mathrm{T}}^{RecoJet}/p_{\mathrm{T}}^{GenJet}$ (response) is recorded in bins of p_{T}^{GenJet}. The mean value of the response distribution is an estimator of the true response and is used to calculate the jet calibration factors as a function of the raw reconstructed jet p_{T} and η. The Monte Carlo truth correction varies significantly between the different jet types and can be seen elsewhere [1]. For CALO jets, the correction factor ranges from 2.5 at $p_{\mathrm{T}} = 30\,\mathrm{GeV}$ to 1.1 at $p_{\mathrm{T}} = 2\,\mathrm{TeV}$. For JPT jets, the correction factor is less than 1.1 for the entire p_{T} range in the region $|\eta| < 1.8$ while it rises up to 1.4 in the region $1.8 < |\eta| < 3$. For PF jets with $p_{\mathrm{T}} > 30\,\mathrm{GeV}$, the correction factor is 1.1 in the central region $|\eta| < 1.3$ and rises slightly up to 1.2 in the other η regions. The correction factor for all jet types, outside the tracker coverage ($|\eta| > 2.6$) is similar, ranging from 1.2 at $p_{\mathrm{T}} = 20\,\mathrm{GeV}$ to 1.05 at $p_{\mathrm{T}} = 200\,\mathrm{GeV}$.

3 Relative Jet Energy Scale vs η

3.1 Methodology and Event Selection

The Monte Carlo truth calibration is applied to all reconstructed jets (corrected jets) and removes the η and p_{T} dependence of the average jet energy response. In order to confirm the independence of the relative corrected jet energy response on η, the dijet p_{T} balance technique is employed. This technique was first used at SPPS [8], and later refined by Tevatron experiments [9, 10]. A detailed description of the feasibility study of the method in CMS is given in [11]. The method is based on the transverse momentum conservation and utilizes the p_{T} balance in back-to-back dijet events with one jet (barrel jet) in the central control region of the calorimeter, $|\eta| < 1.3$, and the other jet (probe jet) at arbitrary η. The central region is chosen as reference because of the uniformity of the detector [12], the small variation of the jet energy response and since it has the highest jet transverse momentum reach.

To collect an unbiased dijet calibration sample, CMS employs dedicated High Level Triggers which fire on the average uncorrected $p_{\mathrm{T}} = (p_{\mathrm{T}1} + p_{\mathrm{T}2})/2$ of the two leading jets above the thresholds of 15 GeV, 30 GeV and 50 GeV respectively. The effective integrated luminosity of each trigger path used in the dijet p_{T} balancing method is 0.05, 0.35 and $2.9\,\mathrm{pb}^{-1}$ respectively.

At offline, events are required to contain at least two jets; one of them being in the barrel region of $|\eta| < 1.3$. In addition, all jets are calibrated using the Monte Carlo truth jet energy corrections. To enrich the sample in $2 \to 2$ process, the two leading jets must be azimuthally separated by $\Delta\phi > 2.7$. Furthermore, no additional jets with $p_{\mathrm{T}}^{3rdJet}/p_{\mathrm{T}}^{dijet} > 0.2$ are allowed, where $p_{\mathrm{T}}^{dijet} = (p_{\mathrm{T}}^{probe} + p_{\mathrm{T}}^{barrel})/2$ is the average p_{T} of the two leading jets.

In the selected event sample we study the distribution of the balance quantity:

$$B = \frac{p_{\mathrm{T}}^{probe} - p_{\mathrm{T}}^{barrel}}{p_{\mathrm{T}}^{dijet}} \tag{2}$$

in bins of $|\eta^{probe}|$ and p_{T}^{dijet}. In order to avoid a trigger bias, only the highest threshold, fully efficient trigger path contributes in each p_{T}^{dijet} bin.

The average value of the B distribution, $\langle B \rangle$, in a given $|\eta^{probe}|$ and p_{T}^{dijet} bin is used to determine the relative response:

$$R(\eta^{probe}, p_{\mathrm{T}}^{dijet}) = \frac{2 + \langle B \rangle}{2 - \langle B \rangle} \tag{3}$$

The R variable defined above is mathematically equivalent to $\langle p_{\mathrm{T}}^{probe} \rangle / \langle p_{\mathrm{T}}^{barrel} \rangle$ for narrow bins of p_{T}^{dijet}. The choice of the p_{T}^{dijet} binning minimizes the resolution bias effect (as opposed to binning in p_{T}^{barrel} which leads to maximal bias). Due to the steeply falling jet p_{T} spectrum and the finite energy resolution, each reconstructed jet p_{T} bin is contaminated with true (particle level) jets of lower p_{T} whose detector response fluctuated high. As a result, the measured response is systematically higher. By using the p_{T}^{dijet} as the binning variable, the response fluctuations of the barrel and the probe jets are cancelled on average. If the energy resolution of the barrel and probe jets is the same, the cancellation is perfect while in the general case the cancellation is partial.

3.2 Results and Uncertainties

Data observations are compared to Monte Carlo expectations extracted from QCD events generated with PYTHIA and processed with the full, GEANT 4 based, CMS detector simulation. Figures 1, 2 and 3 show the relative response R for CALO, JPT and PF jets respectively, as a function of $|\eta|$ in three different p_{T}^{dijet} bins. Measurements of R from positive and negative η bins are consistent within the available statistics, and are therefore combined to reduce the statistical uncertainty.

The measured relative response in the Monte Carlo should be ideally equal to unity. The deviation from unity is due to the resolution bias effect described previously which is inherent in the dijet p_{T} balancing method. The finite jet energy resolution, which is in principle different between the barrel jet and the probe jet, and the steeply falling jet p_{T} spectrum lead to a biased measurement of the relative response. The effect is more pronounced at higher values of $|\eta|$ where the resolution difference with respect to the control region is larger.

The measured relative response in the data agrees well with the simulation in $|\eta| < 1.5$ and a small deviation, up to 10% is observed at higher η. The effect is observed for all jet types and is attributed to the higher single particle response in data compared to the simulation [13]. In order to account for the observed shift in the data, an additional residual correction is applied on top of the Monte Carlo truth calibration. The residual correction is equal to the difference between the relative response in data with respect to the Monte Carlo after extrapolating to zero third jet activity and is found to be independent of the jet p_{T}. Figure 4 shows the magnitude of the residual correction for all jet types.

The dominant uncertainties of the residual calibration are due to the available statistics and the resolution bias modeling in the simulation. The resolution bias uncertainty is caused by the uncertainty on the jet p_{T} spectrum and the jet energy resolution in the Monte Carlo. In order to extract a quantitative estimate, the jet p_{T} slope is varied by $\pm 5\%$ and the jet energy resolution is varied by $\pm 10\%$, $\pm 20\%$ and $\pm 25\%$ in the regions $|\eta| < 1.3$, $1.3 < |\eta| < 3$ and $|\eta| > 3$ respectively. In addition, a small systematic uncertainty is attributed to the extrapolation to zero third jet activity. Despite the fact that the residual correction itself is independent of the jet p_{T}, its uncertainty does depend on the jet p_{T}. Figure 5 shows the uncertainty of the residual correction, as a function of $|\eta|$, for two characteristic jet p_{T} values (50 GeV and 200 GeV). As expected, the uncertainty is small ($\leq 2\%$) in the region $|\eta| < 1.3$ and gradually growing for outer $|\eta|$. Currently, the measurement is statistically limited in the high-p_{T} region while statistics and resolution bias are equally contributing in the low-p_{T} extrapolation. The excursions

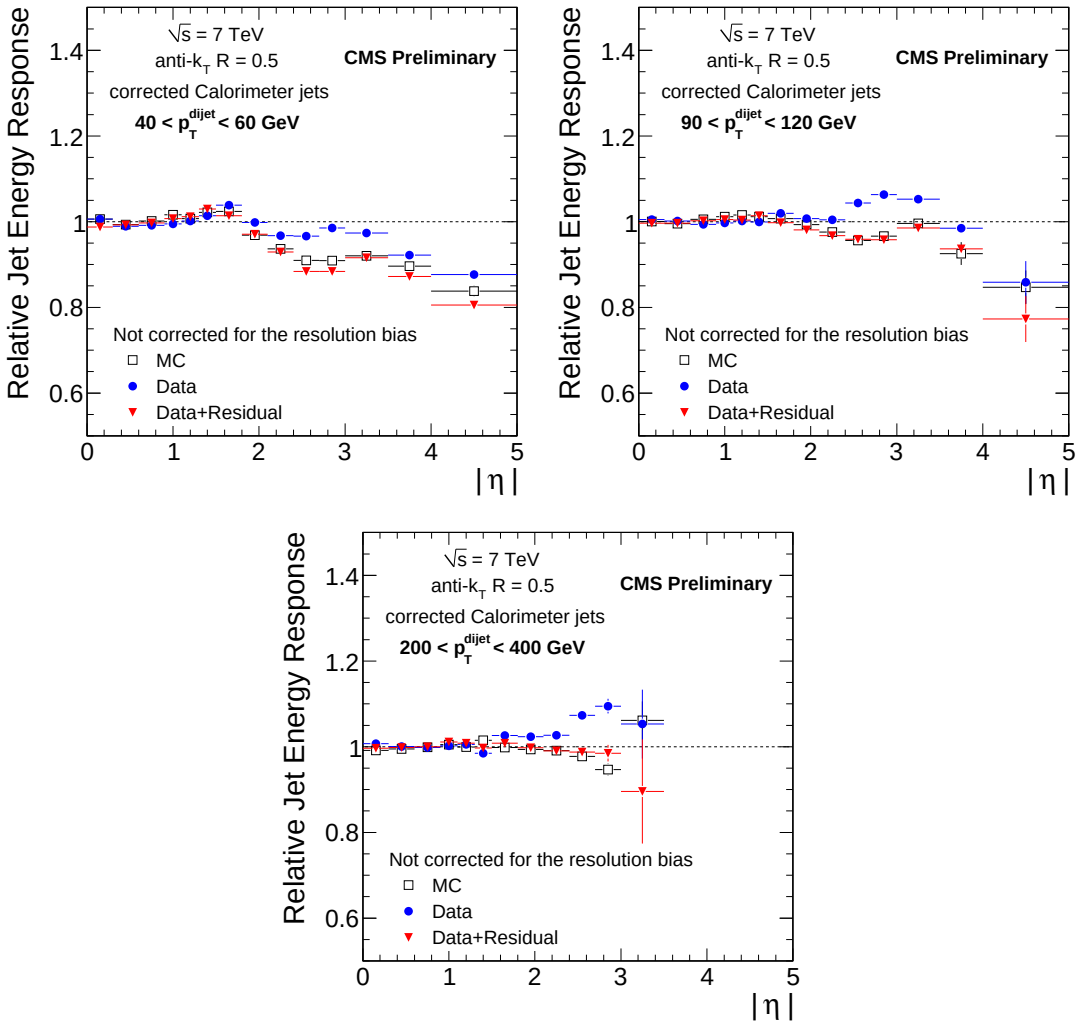

Figure 1: Relative response, R for CALO jets in various p_{T}^{dijet} bins. Open squares: simulation, solid circles: data, solid triangles: data corrected with the residual calibration.

of the uncertainty as a function of $|\eta|$ are driven by the statistical uncertainty in these regions, which is in general not the same for the different jet types.

Figure 6 shows the average relative response ratio between data and simulation. The average is over all the p_{T}^{dijet} bins and is justified by the fact that the difference between data and simulation is approximately independent of p_{T}^{dijet}. Figure 6 also shows the data before and after the residual correction. The resulting comparison between the corrected data and the simulation is consistent with unity within the uncertainty (calculated at jet $p_{\mathrm{T}} = 100\,\mathrm{GeV}$). The non-smooth shape of the uncertainty is caused by the combination of the worse resolution modeling at the detector boundaries and the statistical fluctuations of the in-situ measurement.

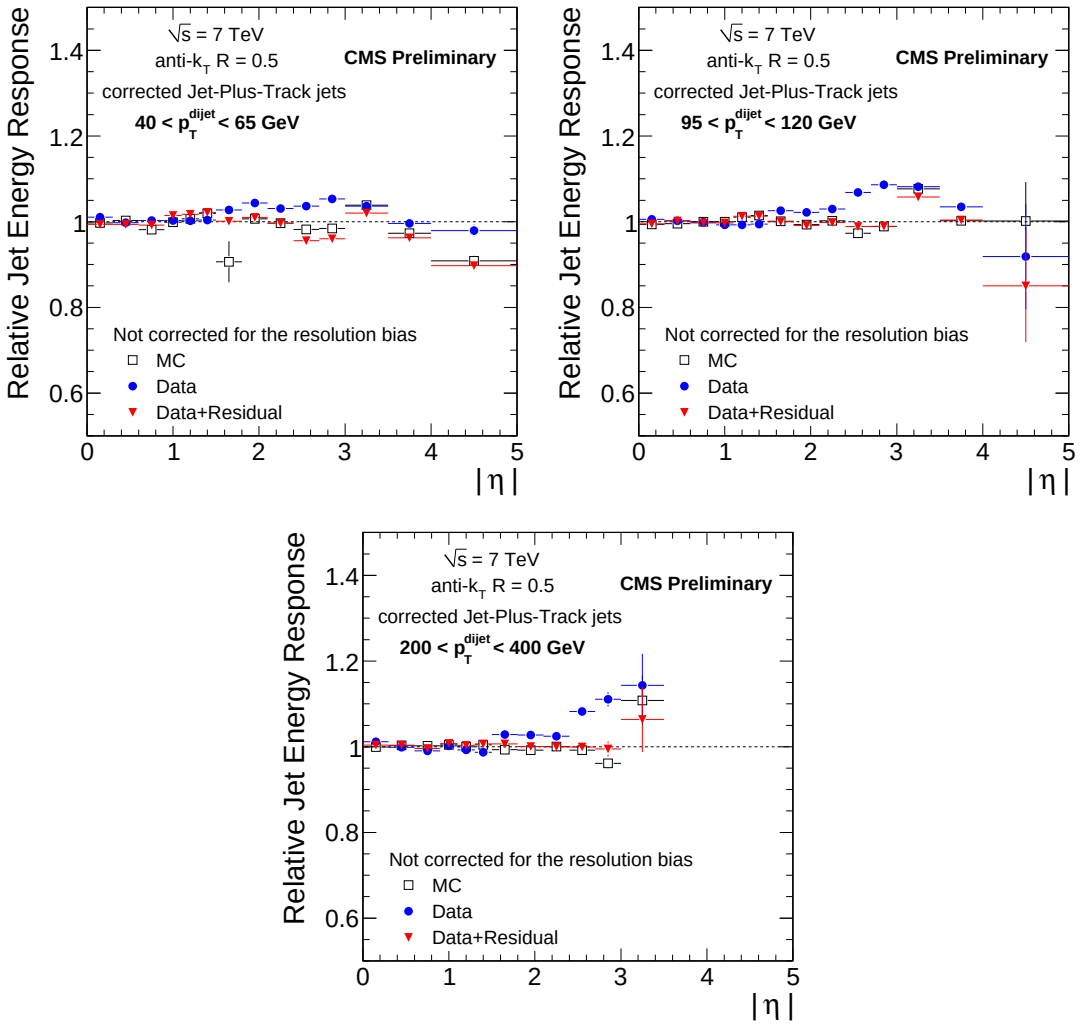

Figure 2: Relative response, R for JPT jets in all p_{T}^{dijet} bins. Open squares: simulation, solid circles: data, solid triangles: data corrected with the residual calibration.

4 Absolute Jet Energy Scale

4.1 Methodology and Event Selection

The absolute jet energy response is measured in the reference region $|\eta| < 1.3$ using γ+jet events, with two different methods: the MPF (missing E_T projection fraction) and the p_{T} balance. Both methods exploit the balance in the transverse plane between the photon and the recoiling jet. The photon is used as a reference object because it is accurately measured in the crystal electromagnetic calorimeter (ECAL).

The MPF method (extensively used at the Tevatron [9]) starts from the fact that the γ+jet events have no intrinsic missing E_T and that the photon is perfectly balanced by the hadronic recoil in the transverse plane:

$$\vec{p}_{\mathrm{T}}{}^{\gamma} + \vec{p}_{\mathrm{T}}{}^{recoil} = 0 \tag{4}$$

For reconstructed objects, this equation can be rewritten as

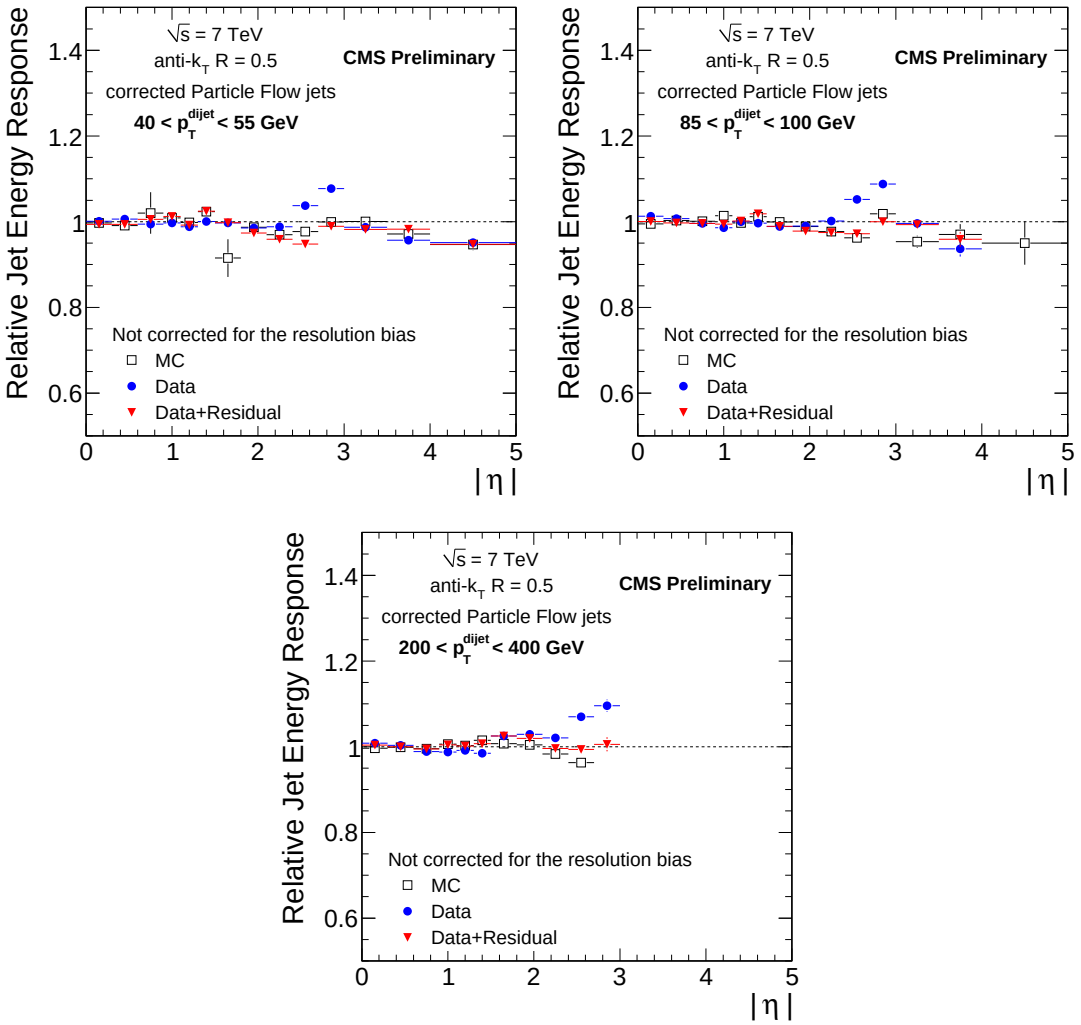

Figure 3: Relative response, R for PF jets in various p_{T}^{dijet} bins. Open squares: simulation, solid circles: data, solid triangles: data corrected with the residual calibration.

$$R_{\gamma}\vec{p}_{\mathrm{T}}{}^{\gamma} + R_{recoil}\vec{p}_{\mathrm{T}}{}^{recoil} = -\vec{E}_T^{miss} \tag{5}$$

where R_{γ} and R_{recoil} are the detector responses to the photon and the hadronic recoil.

Solving the two equations for R_{recoil} gives:

$$R_{recoil} = R_{\gamma} + \frac{\vec{E}_T^{miss} \cdot \vec{p}_{\mathrm{T}}{}^{\gamma}}{(p_{\mathrm{T}}^{\gamma})^2} \equiv R_{MPF} \tag{6}$$

This equation forms the definition of the MPF response R_{MPF}. The additional step needed is to extract the true jet response from the measured MPF response. In general, the recoil consists of additional jets, beyond the leading one, soft particles and unclustered energy. The relation $R_{leadjet} = R_{recoil}$ holds to a good approximation if the particles that are not clustered into the leading jet, have a response similar to the ones inside the jet, or if these particles are in a direction perpendicular to the photon axis. Small response differences are irrelevant if most of the

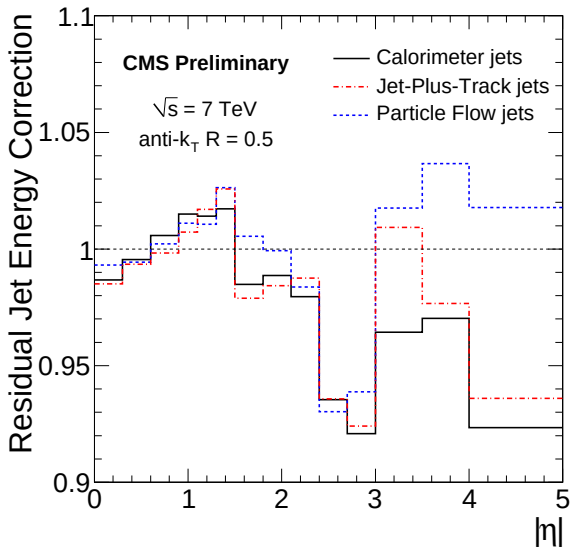

Figure 4: Final residual correction for all jet types, after extrapolation to zero 3rd jet p_{T}.

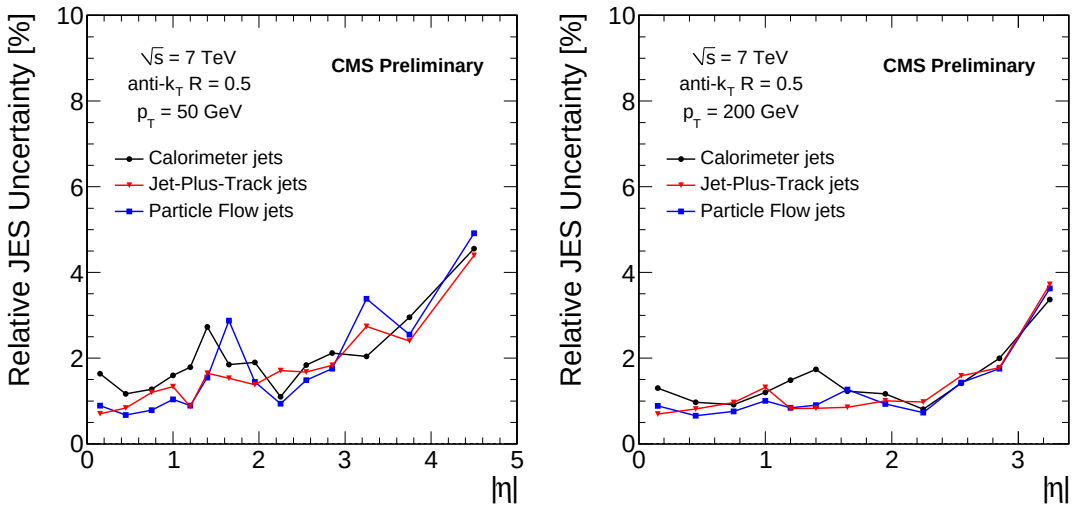

Figure 5: Uncertainty of the residual correction for fixed jet p_{T}.

recoil is clustered into the leading jet. This is ensured by vetoing secondary jets in the selected back-to-back γ+jet events.

The p_{T} balancing method uses the ratio between the jet and the photon p_{T} as an estimate of the jet response: $R_{leadjet} = p_{\mathrm{T}}^{jet} / p_{\mathrm{T}}^{\gamma}$. The technique was introduced by the Tevatron experiments [9, 10]. A detailed feasibility study of the method for CMS is described in [14].

The MPF method is less sensitive to various systematic biases compared to the p_{T} balancing method, as will be discussed later. It is particularly well suited for PF jets due to the superior resolution of the PF missing E_T. The MPF is used in CMS as the main method to measure the energy response, while the p_{T} balancing is used to facilitate better understanding of various systematic uncertainties and to perform cross-checks.

The High Level single photon triggers above the 10 GeV and 15 GeV p_{T} thresholds are used

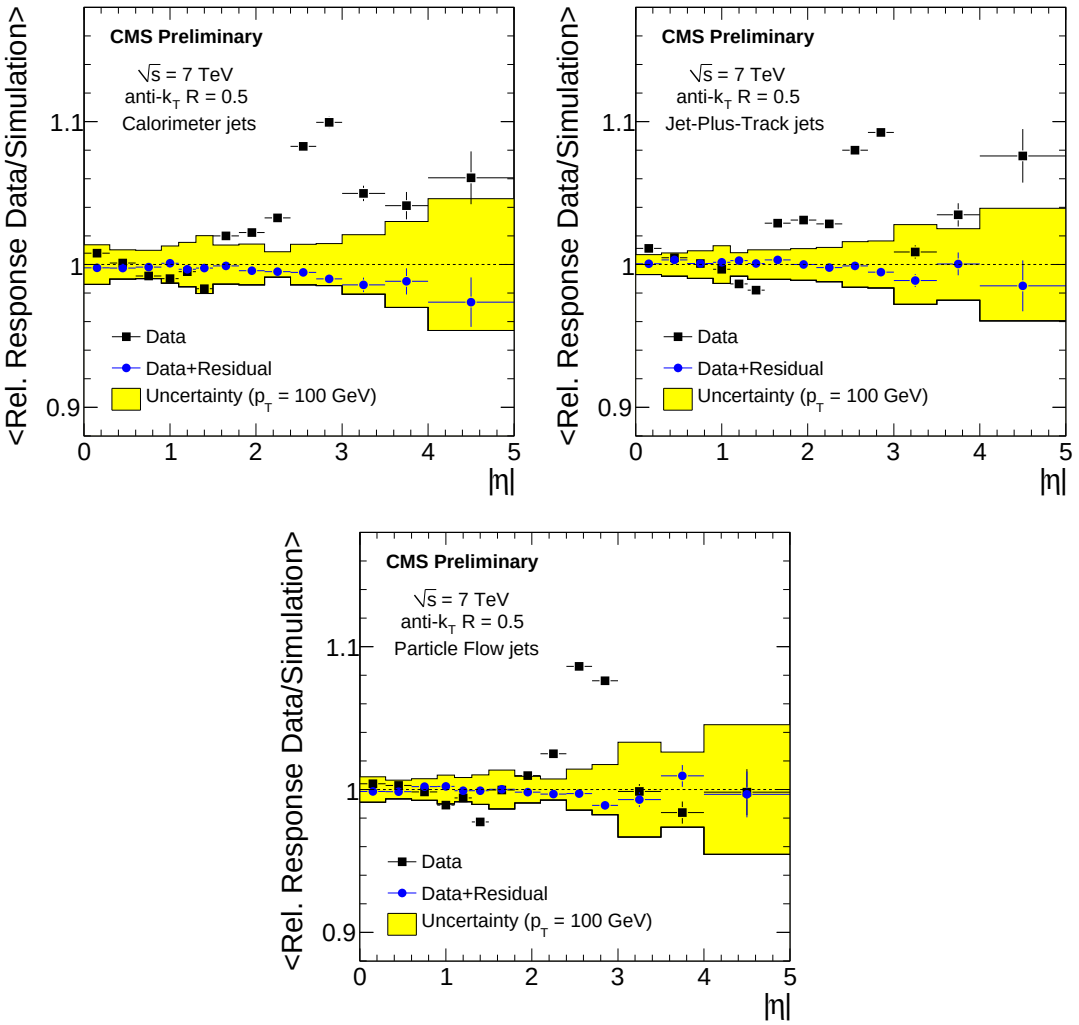

Figure 6: Average relative response ratio between data and simulation for all jet types. The data are shown before (solid squares) and after (solid circles) the residual correction and are compared to the uncertainty of the measurement.

to collect the γ+jet sample. The data analyzed correspond to the integrated luminosity of $L_{int} = 2.9\,\mathrm{pb}^{-1}$. At offline, photon candidates are required to have $p_{\mathrm{T}}^{\gamma} > 15\,\mathrm{GeV}$ within the barrel region of ECAL, $|\eta| < 1.3$. The photon candidates must be isolated in the hadron calorimeter (HCAL), in the ECAL and in the tracker, and have a shower shape consistent to that of a photon [1]. In the selected photon sample, the presence of a barrel jet ($|\eta| < 1.3$) recoiling against the photon candidate in azimuth by $\Delta\phi > 2.7$ is required. To reduce the effect of initial and final state gluon radiation that violates jet-photon p_{T} balance, events containing additional jets with $p_{\mathrm{T}}^{\mathrm{jet2}} > 0.2\ p_{\mathrm{T}}^{\gamma}$ and outside the $\Delta R = 0.25$ cone around the photon direction are vetoed. The selected $\gamma + jet$ sample covers the p_{T}^{γ} range from 15 GeV to $\sim 200\,\mathrm{GeV}$.

The γ+jet Monte Carlo sample consists of events generated with PYTHIA and processed with the full, GEANT 4 CMS detector simulation.

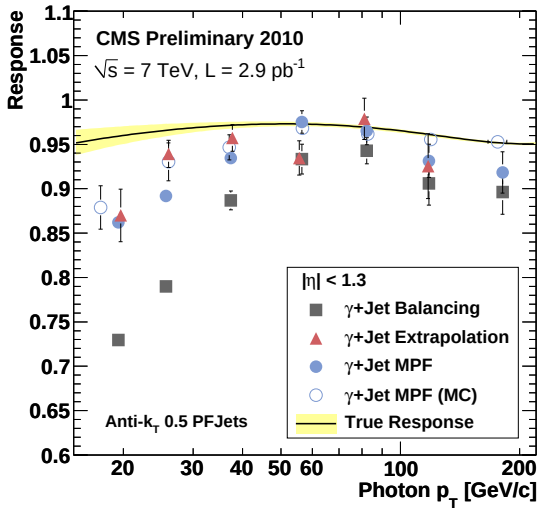

Figure 7: Measured response of PF jets versus p_{T}^{γ} from the MPF method, the p_{T} balancing method, and the p_{T} balancing with $p_{\mathrm{T}}^{\mathrm{jet2}} \to 0$ extrapolation. The Monte Carlo MPF-based and truth response are also shown.

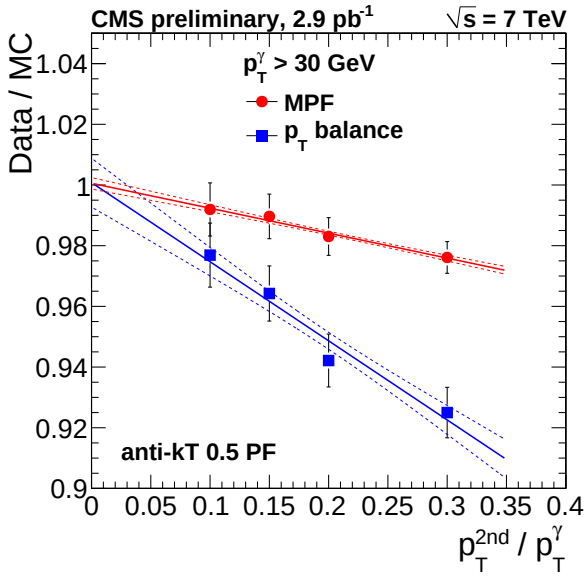

Figure 8: Data/Monte Carlo response ratio for MPF and p_{T} balance methods as a function of the p_{T} threshold on secondary jet.

4.2 Results and Uncertainties

Figure 7 shows the response extracted from the MPF and p_{T} balancing methods as a function of p_{T}^{γ}. It also shows the true response obtained from γ+jet Monte Carlo events, as a mean value of the p_{T} ratio of reconstructed jet and its spatially matched generator jet, $\langle p_{\mathrm{T}}^{Jet} / p_{\mathrm{T}}^{GenJet} \rangle$. The measured jet response is systematically lower than the true jet response. This effect is caused by the presence of additional jets (below the $p_{\mathrm{T}}^{\mathrm{jet2}} = 0.2\ p_{\mathrm{T}}^{\gamma}$ threshold) in the event which spoil the idealized topology of a jet recoiling against a photon. In the p_{T} balancing method,

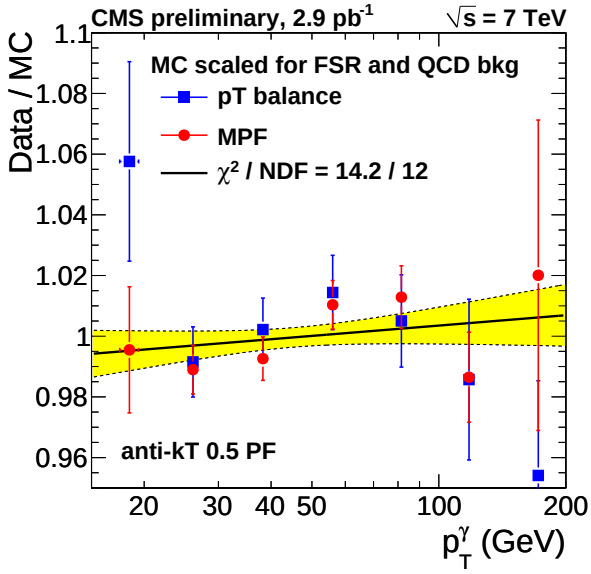

Figure 9: Data/Monte Carlo ratio of reponse from the MPF and the p_{T} balance methods. The optimal fit to both sets of data is shown with the statistical uncertainty band superimposed.

the secondary jet effect is more pronounced because it affects directly the transverse momentum balance between the photon and the leading jet. In the MPF method, the presence of the secondary jet(s) affects the measurement to a lesser extent and mainly through the response difference between the leading jet and the secondary softer jet(s). To remove the observed bias, the response measurements are repeated with decreasing values of the threshold on the second jet p_{T}. The measurement is then extrapolated to the $p^{\mathrm{jet2}}_{\mathrm{T,max}} = 0$ value. Figure 8 shows the data/Monte Carlo ratio, relative to the ECAL scale, for MPF and p_{T} balance as a function of the upper cut on the secondary jet p_{T}. The data/Monte Carlo ratio is less than one for loose veto cuts on the secondary jet pt, but extrapolates linearly to unity with $p^{\mathrm{jet2}}_{\mathrm{T}} \to 0$ for both methods.

Figure 9 shows the data/Monte Carlo response ratio after the extrapolation to $p^{\mathrm{jet2}}_{\mathrm{T,max}} = 0$ for both MPF and p_{T} balancing methods. The two measurements are statistically un-correlated to a good approximation and the two sets of points are fitted together by the log-linear function shown in the figure. The fit gives data/Monte Carlo = $0.993 \pm 0.004(\mathrm{stat.}) \pm 0.026(\mathrm{syst.})$ at $p_{\mathrm{T}} = 50\,\mathrm{GeV}$, relative to the ECAL scale. The measured points are also consistent with the no p_{T} dependence assumption.

In addition to the γ+jet sample, the absolute jet energy scale can also be measured from the Z+jet sample. The currently available statistics do not allow for an accurate measurement but this will be possible with $\sim 40\,\mathrm{pb}^{-1}$ of integrated luminosity. Preliminary estimates indicate that the absolute jet energy scale measured from the Z+jet sample is consistent with the result from the γ+jet sample, to within 4% statistical uncertainty.

Once the jet energy scale is established precisely for PF jets, the estimated uncertainties are transfered to the other jet types. This is done by direct jet-by-jet comparision between different jet types in the QCD dijet sample. The PF and CALO (JPT) jets are spatially matched in the η, ϕ plane by requiring $\Delta R = \sqrt{(\Delta\eta)^2 + (\Delta\phi)^2} < 0.25$. For the matched jet pairs the relative response of CALO (JPT) jets $p_{\mathrm{T}}^{CALO}/p_{\mathrm{T}}^{PF}$ ($p_{\mathrm{T}}^{JPT}/p_{\mathrm{T}}^{PF}$) is measured as a function of p_{T}^{PF}. The study is described in detail in [1], where an excellent data/Monte Carlo agreement is observed, at the level of 0.5% in the relative response between the jets types. This indicates that the preci-

sion of the CALO and JPT calibration is comparable to that of the PF jets. The observed 0.5% level of data/Monte Carlo agreement is taken into account as an additional residual systematic uncertainty for CALO and JPT jets.

The uncertainty of the absolute jet energy scale measurement has five main components: uncertainty in the MPF method, photon energy scale, extrapolation to high p_T, offset due to noise and pile-up at low p_T, and the Monte Carlo truth residuals that are not corrected for.

The MPF method uncertainty. The MPF method is affected by several small uncertainties that mainly contribute at low p_T: flavor mapping, parton correction, QCD background, secondary jets and proton fragments. The various contributions are shown in Fig. 10.

The flavor mapping uncertainty accounts for the response difference between jets in the quark-rich photon+jet sample used to measure the absolute jet energy scale, and those in the gluon-rich QCD sample. This is estimated from the simulation, where the jet response in the QCD dijet sample is compared to the one from the photon+jets sample. The 50% of the observed difference is taken as an estimate of the flavor mapping systematics and amounts to $\sim$ 1% uncertainty.

The parton correction uncertainty is estimated from the simulation by using jets reconstructed with larger size parameter ($R = 0.7$) and comparing the extrapolation to the zero secondary jet activity with respect to the nominal size parameter ($R = 0.5$).

The dominant background for photon+jets events is the QCD dijet production where one leading jet fragments into a hard isolated $\pi^0 \rightarrow \gamma + \gamma$. Such events can alter the measured p_T balance because the leading neutral π^0 carries only a fraction of the initial parton energy. The QCD background uncertainty is estimated by repeating the measurement with two different sets of photon identification and is found to be negligible, compared to the current statistical precision.

The proton fragments are estimated to contribute a fraction of the bias in the MPF method observed in Monte Carlo at $p_T < 30\,\text{GeV}$, by carrying some of the initial momentum outside the detector coverage at $|\eta| > 5$ (the rest of the bias would be mostly underlying event and out-of-cone radiation). The uncertainty is estimated as 50% of the total bias due to the beam fragments.

The secondary jet activity is found to be significantly different between data and Monte Carlo, and it is corrected by extrapolating the data/Monte Carlo ratio for the MPF and p_T balance methods to zero secondary jet activity. The uncertainty is estimated as half of the bias correction applied to the MPF method, leading to 0.8% uncertainty.

Photon scale uncertainty. The MPF and p_T balancing methods are directly sensitive to the uncertainty in the energy of the photon used as a reference object. The photon scale uncertainty is estimated to be $\sim$ 1% based on studies presented elsewhere [15].

High-p_T extrapolation. The current size of the photon+jet sample used to constrain the absolute jet energy scale allows access to a small range of jet p_T between 15 GeV and $\sim$ 200 GeV. In order to study the TeV range already probed by QCD jet physics, it is necessary to estimate the uncertainty of the high p_T extrapolation. While the Monte Carlo response can be scaled to data at the low p_T range, the extrapolation to the high p_T region relies solely on the simulation. The high p_T extrapolation uncertainty is determined by the single pion response and the modeling of the jet fragmentation. The single pion response measurement is presented in [13], where the data is in agreement with the simulation within 3%. The impact on the Monte Carlo truth jet energy scale from a 3% shift in the single pion reponse is estimated by modifying the single

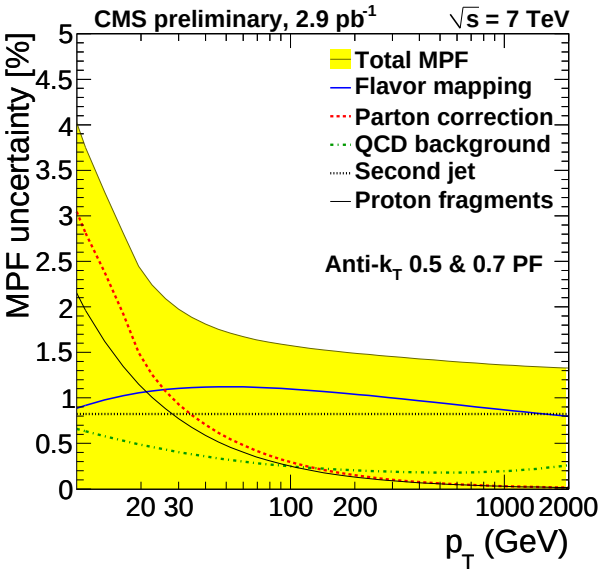

Figure 10: Jet energy scale uncertainty in the MPF method for PF jets.

pion response in the simulation and comparing the obtained jet energy scale to the one with the nominal settings. This leads to about 0.5% uncertainty at $p_T = 2$ TeV for CALO jets, 1% for JPT jets and 1.5% for PF jets. The uncertainty in the jet fragmentation modeling is estimated by two independent fragmentation models (PYTHIA and Herwig++ [16]), leading to an uncertainty of about 4% at $p_T = 2$ TeV.

Offset uncertainty. The average pile-up in the current dataset amounts to one additional collision per event. While the effect is small and does not require a dedicated offset correction, it contributes to the jet energy scale uncertainty at low p_T. The measured absolute calorimeter offset is 0.2 GeV per pile-up event [1], consistent with Monte Carlo expectations. At $p_T = 30$ GeV it leads to an 1.5% uncertainty for CALO jets and 0.8% for JPT and PF jets.

Residuals. The residuals are considered as an uncertainty in order to take into account imperfections in the original Monte Carlo truth jet energy calibration. These are estimated to be 1.5% for CALO jets, 2% for JPT jets and 1% for PF jets.

The summary of the absolute jet energy scale uncertainties is shown in Fig. 11 for the three jet types. The uncertainties vary from 3% to 5% over the p_T range of 30 GeV (20 GeV, 15 GeV) up to 2 TeV for CALO (JPT, PF) jets.

5 Total Jet Energy Correction Factors and Uncertainties

The measurements of the relative and absolute jet energy scales presented in the previous sections indicate that the Monte Carlo truth jet energy calibration is a good starting point: only a small residual correction is required to fix the relative energy scale.

The corrected jet p_T is formally expressed in equation 1, as a function of the raw jet p_T and η where $C(p_T^{raw}, \eta)$ is the combined correction factor. This is composed of the Monte Carlo truth calibration factor $C_{MCtruth}$ (function of p_T^{raw} and η) and the residual calibration $C_{Residual}$ which accounts for the small differences between data and simulation. The two components are applied in sequence as described by the equation below:

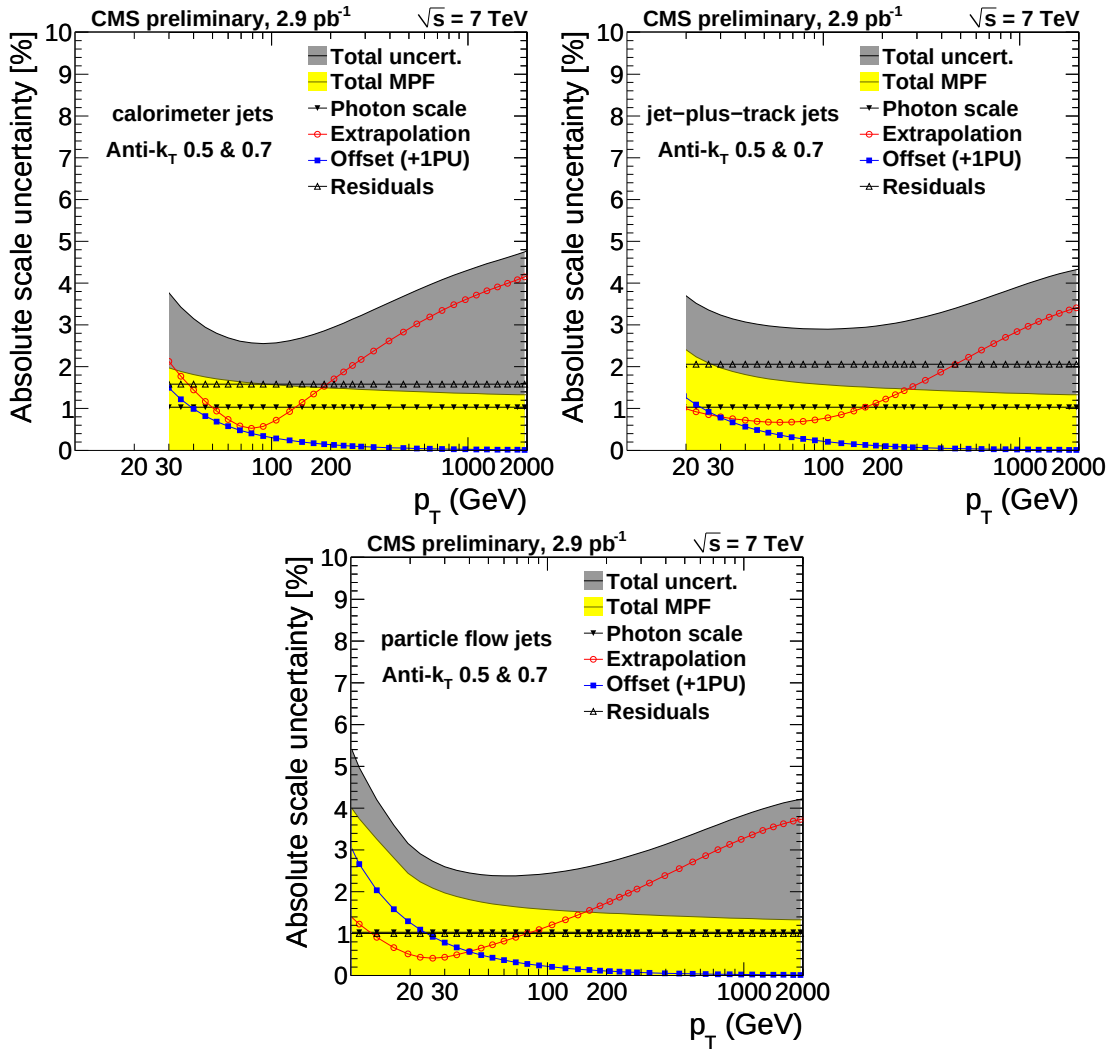

Figure 11: Overall uncertainty on the absolute jet energy scale for CALO jets (a), JPT jets (b) and PF jets (c). The uncertainty for each algorithm is shown down to the lowest recommended p_{T} value.

$$C(p_{\mathrm{T}}^{raw},\eta) = C_{MCtruth}\,(p_{\mathrm{T}}^{raw},\eta) \times C_{Residual}\,(p_{\mathrm{T}}^{raw} \cdot C_{MCtruth}(p_{\mathrm{T}}^{raw},\eta),\eta) \tag{7}$$

The overall jet energy correction factor and its uncertainty is shown in Fig. 12 as a function of η for fixed jet p_{T} values. As expected, CALO jets require a much larger correction factor compared to the track-based algorithms. In the region beyond the tracker coverage, all jet types are in agreement within the systematic uncertainties. Figure 13 shows the correction factors and their uncertainty as a function of the jet p_{T} for fixed η values. The systematic uncertainty of the overall calibration factor is the sum in quadrature of the relative scale and the absolute scale uncertainties. Figure 14 shows the combined uncertainty of the jet energy scale in CMS as a function of jet p_{T} while Fig. 15 shows the same quantity as a function of η.

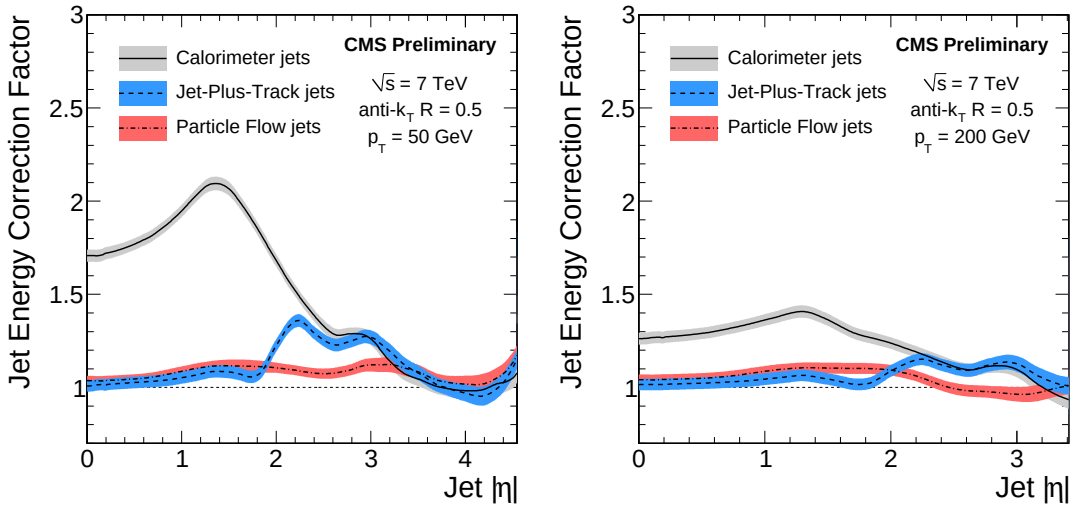

Figure 12: Total jet energy correction factor and its uncertainty (band) as a function of jet η for two jet p_{T} values.

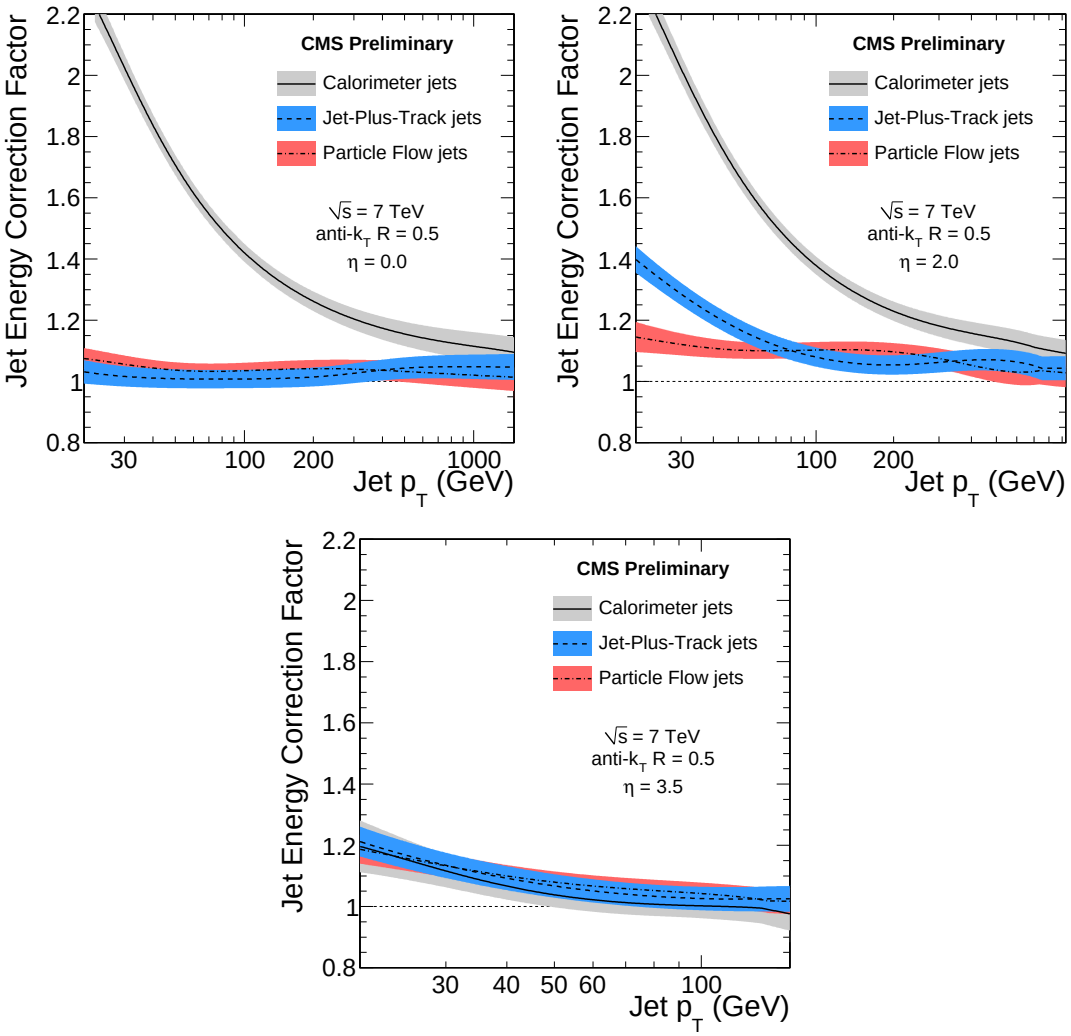

Figure 13: Total jet energy correction factor and its uncertainty (band) as a function of jet p_{T} for different η values.

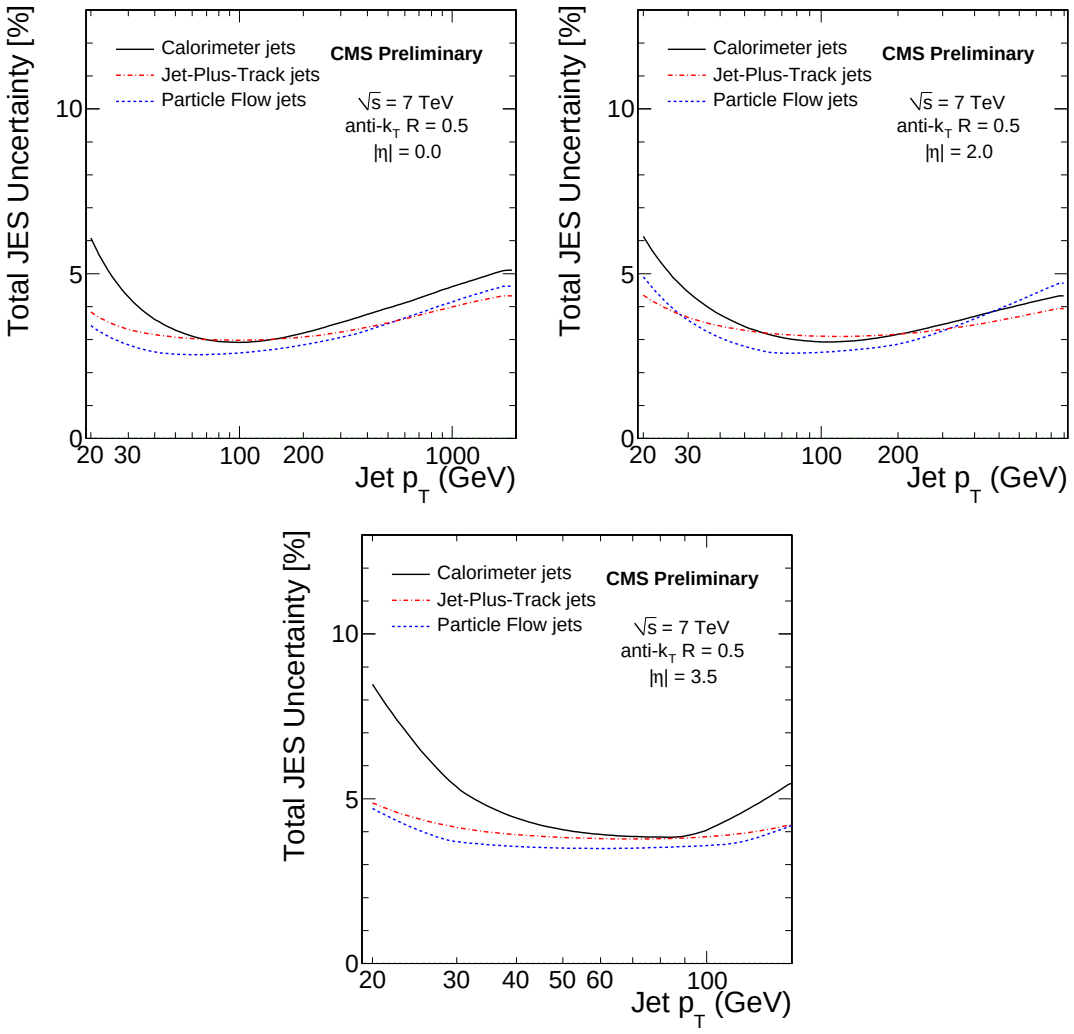

Figure 14: Total jet energy scale uncertainty as a function of jet pt for different η values.

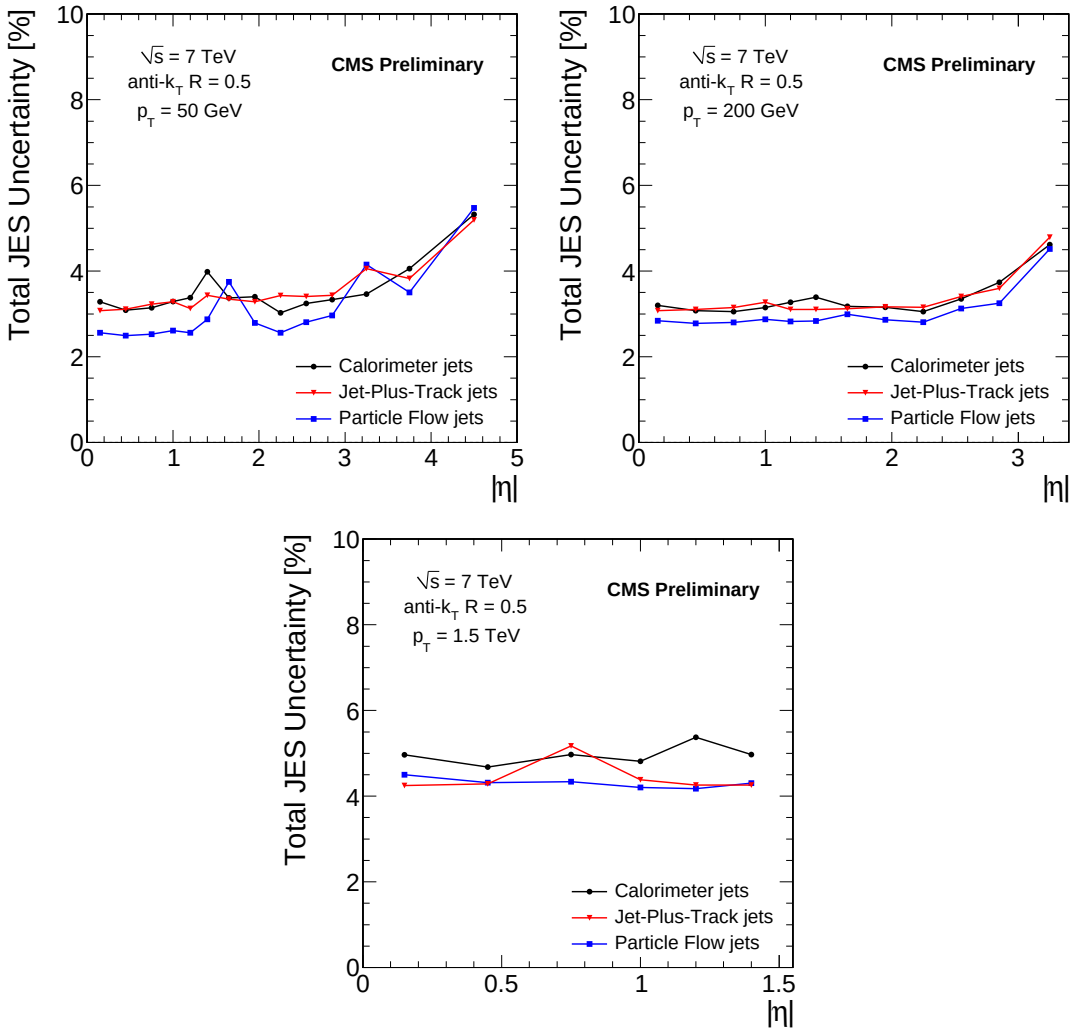

Figure 15: Total jet energy scale uncertainty as a function of jet $|\eta|$ for different jet p_{T} values.

6 Conclusions

The measurement of the jet energy scale in CMS has been presented using $3\,\text{pb}^{-1}$ of data from pp collisions at $\sqrt{s} = 7\,\text{TeV}$. Following the approach of multi-step factorized jet energy calibration adopted by CMS, the relative and absolute jet energy scales have been studied seperately. The dijet p_T balance method has been used to measure the jet energy response as a function of pseudorapidity, relative to the central region ($|\eta| < 1.3$). The MPF and p_T balancing methods have been used to measure the jet energy response in the central region as a function of jet p_T from photon+jet events.

In general, the jet energy scale measurements in data are found to be in agreement with the Monte Carlo predictions. To account for the observed small differences between the two, a residual correction is applied on top of the Monte Carlo truth jet energy calibration.

Detailed studies of the jet calibration precision yield a $3-6\%$ uncertainty of the overall jet energy scale in a wide region of jet p_T from 30 (20, 15) GeV up to 2 TeV for CALO (JPT, PF) jets.

References

[1] CMS Collaboration, "Jet Performance in pp Collisions at $\sqrt{s} = 7$ TeV", *CMS PAS* **JME-10-003** (2010).

[2] CMS Collaboration, "Jet Plus Tracks Algorithm for Calorimeter Jet Energy Corrections in CMS", *CMS PAS* **JME-09-002** (2009).

[3] CMS Collaboration, "Particle-Flow Event Reconstruction in CMS and Performance for Jets, Taus, and E_T^{miss}", *CMS PAS* **PFT-09-001** (2009).

[4] CMS Collaboration, "Commissioning of the Particle-Flow Reconstruction in Minimum-Bias and Jet Events from pp Collisions at 7 TeV", *CMS PAS* **PFT-10-002** (2010).

[5] M. Cacciari, G. P. Salam, and G. Soyez, "The anti-kt jet clustering algorithm", *JHEP* **0804:063** (2008).

[6] T. Sjostrand, S. Mrenna, and P. Skands, "PYTHIA 6.4 physics and manual", *JHEP* **05:026** (2007).

[7] S. Agostinelli et al., "Geant 4 – A Simulation Toolkit", *Nucl. Inst. Meth. A* **506** (2003) 250–303. doi:10.1016/S0168-9002(03)01368-8.

[8] UA2 Collaboration, "Measurement of Production and Properties of Jets at the CERN anti-p p Collider", *Z. Phys.* **C20** (1983) 117. doi:10.1007/BF01573214.

[9] D0 Collaboration, "Determination of the absolute jet energy scale in the D0 calorimeters", *Nucl. Inst. Meth. A* **424** (1999) 352–394. doi:10.1016/S0168-9002(98)01368-0.

[10] CDF Collaboration, "Determination of the jet energy scale at the Collider Detector at Fermilab", *Nucl. Inst. Meth. A* **566** (2006) 375–412. doi:arXiv:hep-ex/0510047.

[11] CMS Collaboration, "Determination of the Relative Jet Energy Scale at CMS from Dijet Balance", *CMS PAS* **JME-08-003** (2009).

[12] CMS Collaboration, "The CMS experiment at the CERN LHC", *JINST* **3** (2008) S08003. doi:10.1088/1748-0221/2/08/S08004.

[13] CMS Collaboration, "Single Particle response in the CMS Calorimeters", *CMS PAS* **JME-10-008** (2010).

[14] CMS Collaboration, "Jet energy calibration with photon+jet events", *CMS PAS* **JME-09-004** (2009).

[15] CMS Collaboration, "Electromagnetic calorimeter calibration with 7 TeV data", *CMS PAS* (2010).

[16] M. Bahr et al., "Herwig++ Physics and Manual", *Eur. Phys. J.* **C58** (2008) 639707. doi:doi:10.1140/epjc/s10052-008-0798-9.